Lara-Rodriguez, Gerardo; Cai, Chunpei
Near Continuum Flows Over a Rotating Disk
Brazilian Journal of Physics, vol. 45, núm. 4, agosto, 2015, pp. 431-438
Sociedade Brasileira de Física
São Paulo, Brasil

Braz J Phys (2015) 45:431–438
DOI 10.1007/s13538-015-0333-z

GENERAL AND APPLIED PHYSICS

Near Continuum Flows Over a Rotating Disk

Gerardo Lara-Rodriguez[1] · **Chunpei Cai**[1]

Received: 3 February 2015 / Published online: 5 June 2015

Abstract We analyze the near continuum flow created by a rotating disk facing a stagnant gas. The flow-field properties change from the traditional continuum solutions, due to the introductions of new velocity-slip and temperature-jump boundary conditions. To compute the velocity profiles, a self-similar transformation simplifies the Navier-Stokes equations into a system of ordinary differential equations. The introduction of new boundary conditions generates new parameters which can be adjusted at different degrees of rarefaction. Shooting methods are adopted to solve the differential equations with the new boundary conditions. Based on the solved velocity profiles, exact solutions for the temperature distribution are obtained. The gas temperature at the disk surface shifts towards the free stream temperature, while the heat flux between the gas and surface is reduced. Stream function solutions for the flow at the disk surface are presented to demonstrate the effects of the slip boundary conditions. The torque generated by the disk is obtained with different disk rotating speed, and the gas at the disk surface has different slip velocities.

Keywords Slip flows · Rotating flows · Navier-Stokes equations · Ordinary differential equation · Heat convection

✉ Gerardo Lara-Rodriguez
geralara680@gmail.com

Chunpei Cai
ccai@nmsu.edu

1 New Mexico State University, Las Cruces, NM 88003, USA

1 Introduction

Flows over a rotating disk are highly useful for industrial applications, for example, centrifugal pumps and micropumps [1], turbine blades, viscometry, etc. They are not only limited to the one in the traditional continuum regime, which was already well studied. For example, they are related to material synthetisation [2] and other applications [3–5]. In processes such as chemical vapor deposition [2], a thin film can be synthesized with the use of a rotating disk reactor. The rotating disk contains the substrate that later will be impinged by a chemical mixing. The low pressures often used in this kind of processes increase the mixture mean free path (MFP) [6]. As a consequence, rarefaction effects must be taken into account during the solution of the velocity profiles. Other studies in cooling Micro-Electro-Mechanical-Systems were performed during the past (e.g., Bachok et al. [7]). Moreover, the rotating disk configuration can be used in the study of rotating disk electrodes and in the study of chemical reactions [8].

The solutions to continuum swirling flow over a rotating disk are the most representative exact ones for the Navier-Stokes Equations (NSEs) in three dimensions. The problem was well studied and the solutions involve a symmetrical flow in cylindrical coordinates. A coordinate transformation was introduced by Karman [9] and was also clearly described by White [10], with which the NSEs change from partial differential equations to a system of three Ordinary Differential Equations (ODEs). These new equations can be easily solved with a shooting method, and their solutions include the velocity components. Uncoupled equations for the pressure and temperature can be further solved based on the velocity solutions. A comparison of the viscous effects in flows over a rotating disk was performed in the past by Hannah [11], where the changes in the flow viscosity were analyzed. Sahoo [12] discussed some new progress on solving the Bodewadt flow, which is a twin problem to the rotating disk flow. Also, the entropy change due to velocity-slip and temperature-jump boundary conditions (B.C.s) and the permeability with those B.C.s were also considered in the literature [13]. Metha's [13] work performed some investigations without considerations of the temperature jump conditions, and he adopted a finite difference method to solve for velocity components. Extensions to the case of the two rotating disks were reviewed by Zandberen and Dijkstra [14].

Other than Karman's work, some others worked with different approaches on the rotating disk flows [15–18]. Cochran [15] obtained more accurate results by matching a Talylor series expansion near the disk with a series of solutions, involving exponentially decaying functions far from the disk at the suitable mid point. Benton [16] applied the same approach for unsteady rotating disk flows. Millsaps and Polhausen [17] concentrated on small Prandtl number heat transfer, while Sparrow and Greeg [18] concentrated on high Prandtl number rotating disk flows. Some related discussions including criticism on slip flows over a rotating disk were available in the literature [19–21]. Miklavicic's [19] work emphasized a simplified model for velocity slip flows over a rotating plate by concentrating on mathematic proof, neglecting the temperature effect. Arikoglu [20] used the differential transform method (DTM) introduced by Zhou [22] and obtained different ODEs from Karman [9]. Only the velocity slip along the radial direction was included, without temperature jumps. Pantokratoras [21] pointed out that many works in the literature on solving these ODEs were incorrect due to insufficient of computation length. For example, Osalusi [23] and his coworkers considered many complex rotating disk flow with velocity-slip B.C.s and many other factors including electricity, unfortunately their solution profiles were problematic.

In some applications, such as micropumps [1], rarefaction effects should be considered. The rarefaction effect can be described with the Knudsen number (Kn):

$$Kn = \frac{\lambda}{L}, \tag{1}$$

where λ is the molecule MFP and L is the characteristic length. Rarefied flows can be classified into four regimes: continuum with Kn <0.001, near continuum with $0.001 < Kn < 0.01$, transitional $0.01 < Kn < 10$, and free molecular with $Kn > 10$. The NSEs are applicable in continuum and near continuum regime. The former adopts non-slip and no-jump B.C.s, and the latter shall adopt the velocity-slip and temperature-jump B.C.s [24–26].

This paper aims to further discuss the rarefaction influence on the flowfield solutions. NSEs for incompressible viscous flows will be used, but setting up the B.C.s at the plate surface shall include velocity-slip and temperature-jump.

2 Velocity Distribution of Flows Near a Rotating Disk

As illustrated by Fig. 1, the problem consists of a flat disk rotating at a certain angular velocity ω. Friction is generated by the disk and the outwards flow due to the centrifugal force. The mass flow is sustained by the movement of the flow downwards in the axial direction. Therefore, this problem is a three dimensional flow with rotational symmetry. The suggested solution for the flow near a rotating disk may be obtained from the NSEs:

$$\begin{aligned}
&u\frac{\partial u}{\partial r} - \frac{v^2}{r} + w\frac{\partial u}{\partial z} = -\frac{1}{\rho}\frac{\partial p}{\partial r} + \nu\left(\frac{\partial^2 u}{\partial r^2} + \frac{\partial}{\partial r}\left(\frac{u}{r}\right) + \frac{\partial^2 u}{\partial z^2}\right)\\
&u\frac{\partial v}{\partial r} + \frac{uv}{r} + w\frac{\partial v}{\partial z} = \nu\left(\frac{\partial^2 v}{\partial r^2} + \frac{\partial}{\partial r}\left(\frac{v}{r}\right) + \frac{\partial^2 v}{\partial z^2}\right)\\
&u\frac{\partial w}{\partial r} + w\frac{\partial w}{\partial z} = -\frac{1}{\rho}\frac{\partial p}{\partial z} + \nu\left(\frac{\partial^2 w}{\partial r^2} + \frac{1}{r}\frac{\partial w}{\partial r} + \frac{\partial^2 w}{\partial z^2}\right),
\end{aligned} \tag{2}$$

where u, v, w are considered as the radial, tangential, and axial velocity components. Moreover, the energy conservation is required to describe the fluid heat convection:

$$u\frac{\partial T}{\partial r} + \frac{v}{r}\frac{\partial T}{\partial \theta} + w\frac{\partial T}{\partial z} = \alpha\left(\frac{\partial^2 T}{\partial r^2} + \frac{1}{r}\frac{\partial T}{\partial r} + \frac{1}{r^2}\frac{\partial^2 T}{\partial \theta^2} + \frac{\partial^2 T}{\partial z^2}\right). \tag{3}$$

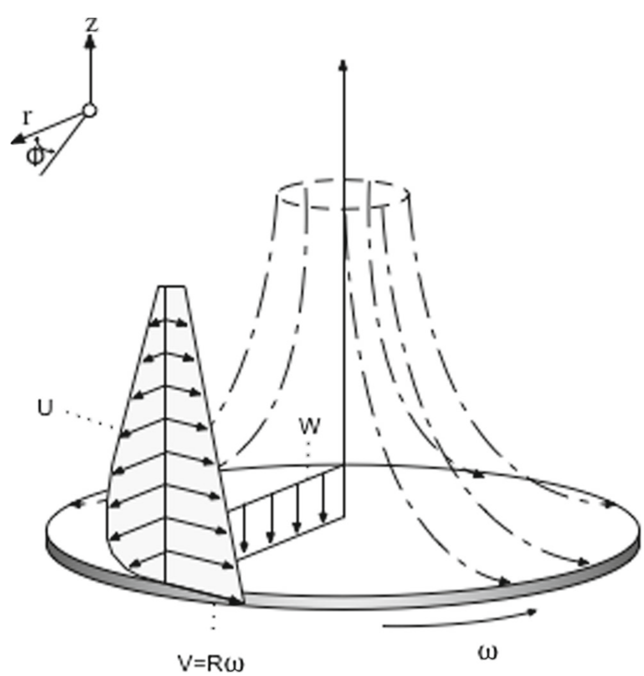

Fig. 1 Illustrations for the problem of flow near a rotating disk

The term of viscous dissipation is neglected; it can be assumed that the gradients of velocity, temperature, and pressure in the axial direction have a larger order of magnitude than those in the radial direction. Besides, flow is considered to be axisymmetric, and the derivatives in the radial and tangential directions are neglected in the case of a disk with a constant surface temperature. With these assumptions, (3) degenerates, as presented by Kendoush [27]:

$$w\frac{\partial T}{\partial z} = \alpha\left(\frac{\partial^2 T}{\partial z^2}\right). \quad (4)$$

In Fig. 1, it is appreciable how the fluid at rest on the top is pulled downwards due to the movement of flow over the disk.

2.1 None Slip and Constant Temperature Surface Conditions (Kn <0.001)

The non-slip B.C.s at the disk surface are:

$$u(r,\theta,0)=0;\ v(r,\theta,0)=r\omega;\ w(r,\theta,0)=0;$$
$$p(r,\theta,0)=0;\ u(r,\theta,\infty)=0;\ v(r,\theta,\infty)=0; \quad (5)$$
$$T(0)=T_w;\ T(\infty)=T_\infty,$$

where r is along the radial direction, ω is the tangential velocity component, and T_w is the temperature at the disk surface. As proposed by Kármán [9], the problem can be reduced to a system of ODEs with the use of a dimensionless parameter, ζ, which is only a function of z. Meanwhile, introductions of F, G, H, and P are required to transform the system of (2):

$$\zeta = z\sqrt{\frac{\omega}{\nu}};\ u=r\omega F(\zeta);\ v=r\omega G(\zeta);$$
$$w=\sqrt{\nu\omega};\ H(\zeta);\ p=\rho\omega\nu P(\zeta), \quad (6)$$

where ν is the kinetic viscosity. In addition, one variable is introduced for the temperature [27]:

$$\Theta = (T-T_w)/(T_\infty - T_w), \quad (7)$$

finally, the system of three differential (2) transforms as follows:

$$2F+H'=0;\ F^2+F'H-G^2-F''=0;$$
$$2FG+HG'-G''=0. \quad (8)$$

The equations for pressure and temperature are,

$$P'-HH'+H''=0, \quad (9)$$

$$\Theta'' = PrH\Theta', \quad (10)$$

where Pr is the Prandtl number. It is noticeable that for this simplified case where the disk surface temperature remains constant, the temperature distribution occurs only as a function of ζ.

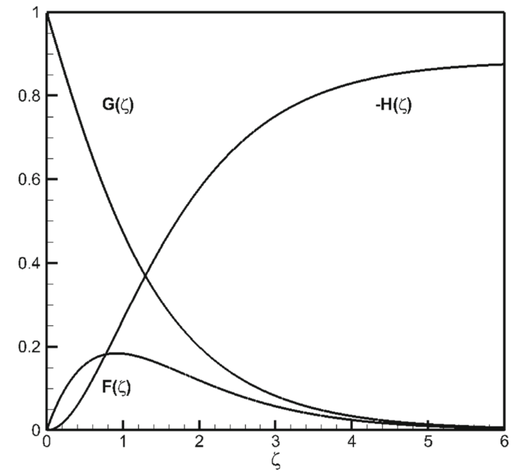

Fig. 2 F(ζ), G(ζ), and H(ζ) with non-slip B.C.s

The rotating disk B.C.s can be transformed to:

$$F(0)=0;\ G(0)=1;\ H(0)=0;\ P(0)=0;$$
$$F(\infty)=0;\ G(\infty)=0;\ \Theta(0)=0;\ \Theta(\infty)=1. \quad (11)$$

It shall be mentioned that the simulation adopted a long integration domain over ζ, but only a shorter interval is displayed, to better illustrate the details. Observations on the farfield and surface solutions confirming the above B.C.s are satisfied; hence, this work does not have issues pointed out by Pantokratoras [21].

The solutions to (8) can be obtained with a numerical shooting method. The solutions are plotted in Figs. 2 and 3. With solved exact solution for H, the temperature solution can be written as:

$$\Theta(\zeta) = \int_0^\zeta e^{Pr\int_0^\zeta H(s)ds}d\zeta \Big/ \int_0^\infty e^{Pr\int_0^\zeta H(s)ds}d\zeta. \quad (12)$$

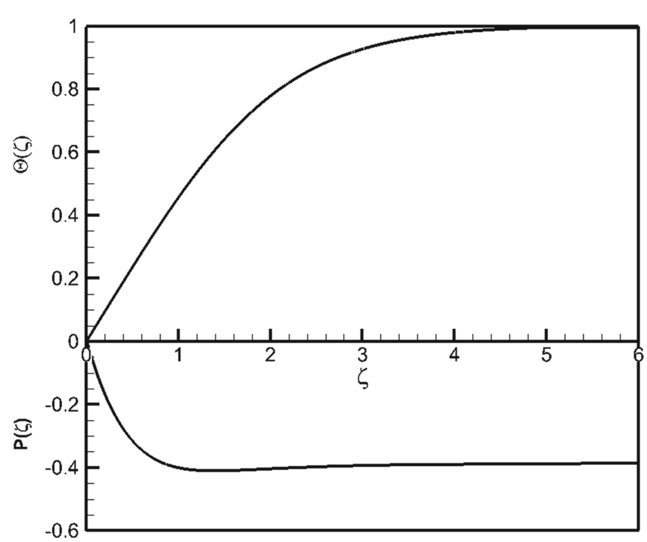

Fig. 3 Similarity solutions for pressure and temperature

2.2 Solutions with the Velocity-Slip B.C.s (0.001< Kn <0.01)

Flows with a small scale or a large MFP present weak rarefaction effect. The solutions for the velocity components in this regime are achievable with adoptions of velocity-slip which can be expressed as:

$$\begin{aligned} u_s(r,\theta,0) &= u_g - u_w = \tfrac{2-\sigma_M}{\sigma_M}\lambda \tfrac{\partial u}{\partial n}|_w; \\ v_s(r,\theta,0) &= v_g - v_w = r\omega + \tfrac{2-\sigma_M}{\sigma_M}\lambda \tfrac{\partial v}{\partial n}|_w; \\ w_s(r,\theta,0) &= 0, \end{aligned} \tag{13}$$

where u_s and v_s are the disk surface slip velocity components, the subscript "$_g$" denotes the the bulk gas velocity at the surface. The velocity components at the plate are denoted by subscript "$_w$", λ is the MFP, σ_M is the momentum accommodation coefficient and can be determined with experiments. Finally the velocity gradients normal to the disk surface are $\partial u/\partial n$ and $\partial v/\partial n$. It shall be pointed out that for the Maxwellian type of B.C.s, there shall be an extra term which contains $\partial T/\partial s$, for u_s and v_s. However, usually their magnitudes are several orders smaller than the velocity gradients. The system of equations remains the same as (8). The transformed B.C.s at the disk surface are:

$$\begin{aligned} F(0) &= \left(\tfrac{2}{\sigma_M} - 1\right)\sqrt{\tfrac{\omega\lambda^2}{\nu}}F'(0); \\ G(0) &= 1 + \left(\tfrac{2}{\sigma_M} - 1\right)\sqrt{\tfrac{\omega\lambda^2}{\nu}}G'(0); \\ H(0) &= 0. \end{aligned} \tag{14}$$

Nguyen [3] reviewed many factors which may affect the surface velocity-slip B.C.s. His work concentrated on micropumps; there is no need to consider temperature-jump, nor the velocity slip along the radial direction. Blanchard [28] investigated many factors which can affect the surface accommodation coefficients as well.

Equation (14) includes a constant $\omega\lambda^2/\nu$ and implies that the slip B.C.s are independent of the surface position, but rather depending on the disk angular velocity. By comparison, the radial and tangential velocity component profiles, which are described in (6), depend on the radial position.

In a similar manner, the temperature-jump B.C. is:

$$T(r,\theta,0) = T_g - T_w = \frac{2-\sigma_T}{\sigma_T}\frac{2\gamma}{\gamma+1}\frac{\lambda}{Pr}\frac{\partial T}{\partial n}|_w. \tag{15}$$

Equations (7) and (15) lead to:

$$\Theta'(0) = c\Theta(0), c = \frac{\sigma_T}{2-\sigma_T}\frac{Pr(\gamma+1)}{2\gamma}\sqrt{\frac{\nu}{\omega\lambda^2}}, \tag{16}$$

and there is an exact solution for the temperature:

$$\Theta(\zeta) = 1 - c\Theta(0)\int_\zeta^\infty e^{Pr\int_0^\zeta H(s)ds}d\zeta, \tag{17}$$

where c is positive. From the same equation we can conclude that $0 < \theta(0) < 1$ because $\Theta'(0)$ is in general positive. Due to this fact, the temperature-jump leads to the gas temperature at the surface to approach the the farfield temperature, T_∞. Using the first order approximation, with the slip and jump B.C.s, the value of $\Theta(\infty) - \Theta(0)$ is smaller than the corresponding value obtained with the non-slip and no-jump B.C.s. As such, it can be projected a weaker heat flux may happen at the object surface. The rotation speed effect on the temperature is included via $H(\zeta)$.

In the literature, higher order of velocity-slip and temperature-jump B.C.s for flows over a rotating disk were also be considered [29, 30].

2.3 Stream Function

As a basic concept in fluid mechanics, the two-dimensional stream function in a cylindrical coordinate is:

$$d\psi = -vdr + rud\theta = 0, \tag{18}$$

with (5), it leads to the following relation:

$$r = k_1\left[\exp\left(\frac{F(0)}{G(0)}\theta\right)\right]. \tag{19}$$

In other words, (19) might be used to describe the behavior of the flow once the similarity solution is achieved. The stream line solution can be obtained analytically and used to describe the influence of the velocity-slip at the disk surface.

2.4 Torque Coefficient

The viscous drag generated by the disk is the only mean that the disk transfers momentum to the fluid that otherwise stays at rest. The circumferential shear stress on the disk is defined as [9]:

$$\tau_{z\theta} = \mu\frac{\partial v}{\partial z}\Big|_{z=0} = \rho r G_0'\sqrt{\nu\omega^3}. \tag{20}$$

Once the value for G_0' is obtained, (20) can be solved analytically for a range of values of r. This equation is further used to define a dimensionless torque coefficient as following,

$$C_m = \frac{-\int_0^{r_o}\tau_{z\theta}r\,(2\pi r dr)}{\rho\omega^2 r_0^5/2} = \sqrt{\frac{(\pi G_0')^2\nu}{r_0^2\omega}}, \tag{21}$$

Equation (21) is an extension of the determination of the total torque to turn a disk of radius r_0. This dimensionless parameter is an indicator for the viscous effects in the circumferential direction [31].

3 Discussions

Equation (8) can be solved numerically with (14) and different values of $\sqrt{\omega\lambda^2/\nu}$. The value of λ is considered constant since the density is relatively constant for most of the near-continuum cases. The pressure and temperature solutions governed by (9) and (10) can be obtained directly with attained $H(\zeta)$.

An exact numerical solution for the stream functions is obtained, after the velocity profiles are available. In the case of nonslip flow where a particle describes circular trajectories at the disk surface, appreciable movement is reflected in the B.C.s from (5). On the other hand, the velocity-slip in slightly rarefied flows creates a spiral movement expelling the particles at the disk surface off the disk center.

In the literature, there are further variable changes (e.g., by Benton [16]) for relatively complex problems; however, recent computation improvement allows the solution more straightforward solutions. The swirling flow is assumed to be air, for this case $Pr = 0.7145$ and $\gamma = 1.4$. For the results presented here, σ_M and σ_T are set to 0.8. It is important that some viscosity and conductive effects are assumed trivial for the temperature.

For this case is mandatory to find the initial values $F'(0)$ and $G'(0)$. The assumptions $F(\infty) = G(\infty) = 0$ [10] are required to solve this problem. Although there are modified simple shooting methods [34], this problem can be addressed with a simple shooting method [32]. As explained by Faragó [35], the method of halving the interval is one of the simplest shooting methods, where two guesses, i.e., s_1 and s_2, provide a fix value of $F'(0) = s$ where $s = 0.5(s_1 + s_2)$. The guesses are improved iteratively, modifying in each step either s_1 or s_2, until the obtained boundary values are similar to the actual boundary values [36]. This process is repeated for each value of $\sqrt{\omega\lambda^2/\nu}$.

Figure 4 compares the non-slip velocity profiles against the velocity-slip ones at $\sqrt{\omega\lambda^2/\nu} = 0.1$. The asymptote for $H(\infty)$ decays. In addition, it is expected that the effects of the disk movement disappear as the velocity-slip increases. The similitude with the previous analysis [33] is satisfactory; however, the velocity-slip B.C.s differ from those presented in the previous studies. If the mass flow rate towards the disk is assumed constant in the far-field, and a cylindrical control volume is settled around the disk with a specific radius, R, then the mass flow rate entering in the far-field is proportional to $H(\infty)$. This mass entering the volume must equal to that exiting the control volume because the asymptote for farfield velocity component $H(\infty)$ are the same as those from non-slip B.C.s. To maintain a constant mass flow rate at higher angular velocities, the value for the radial velocity $H(\zeta)$ at large ζ must decrease to compensate for that near the disk surface. This leads to the conclusion that the velocity peak in the radial direction must shift towards the disk surface; hence, a velocity cross-over with the other profile with non-slip B.C.s must happen. This fact is clearly illustrated by Fig. 4.

While the influence of the disk in the radical velocity component $F(0)$ increases as the rarefaction becomes more significant, the tangential velocity component at the disk $G(0)$ decreases. Figures 5 and 6 illustrate the differences generated in the disk surface $\zeta = 0$. It is appreciable that the effects of $F(\zeta)$ and $G(\zeta)$ become smaller when $\zeta \sim \infty$. The maximum value of $F(\zeta)$ is presented closer to the disk surface as the influence of the slip increases.

Figure 7 illustrates $H(\zeta)$ profiles for different values of $\sqrt{\omega\lambda^2/\nu}$. The asymptote for $H(\infty)$ decreases as the flow rarefaction increases. It is appreciable that the influence of the disk effects to the flow becomes insignificant at higher values of ζ in the velocity-slip solutions.

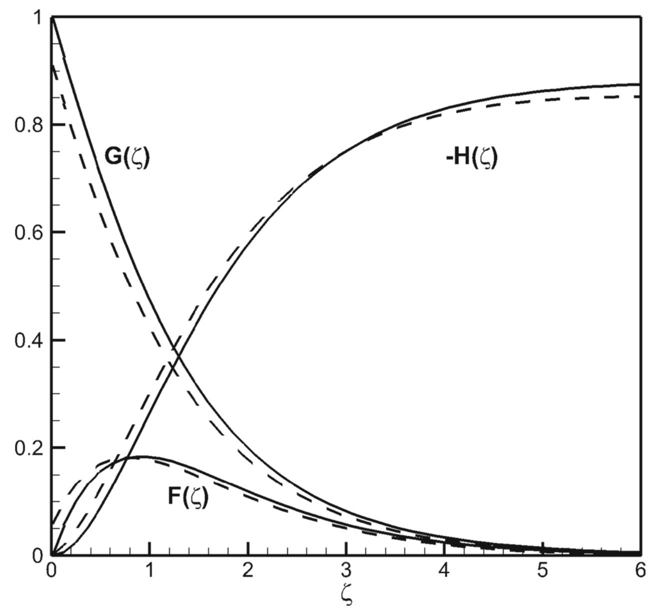

Fig. 4 Comparison of the velocity profiles between the nonslip flow v.s. slip flow with $\sqrt{\omega\lambda^2/\nu} = 0.1$

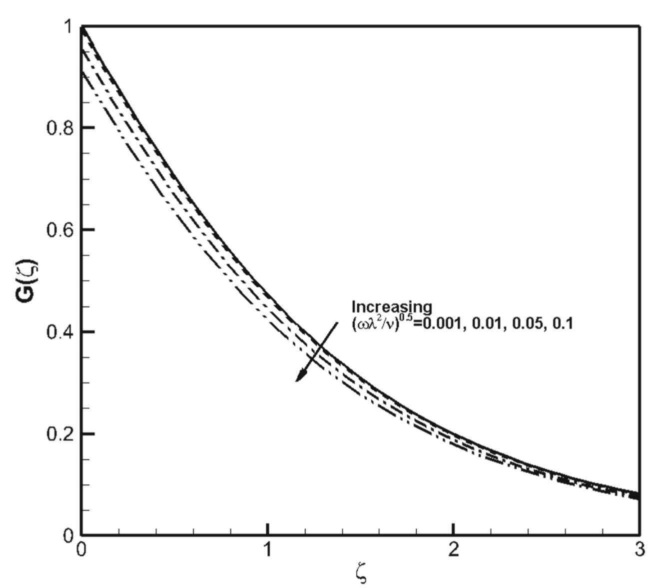

Fig. 5 Tangential velocity profiles with various slip B.C.s

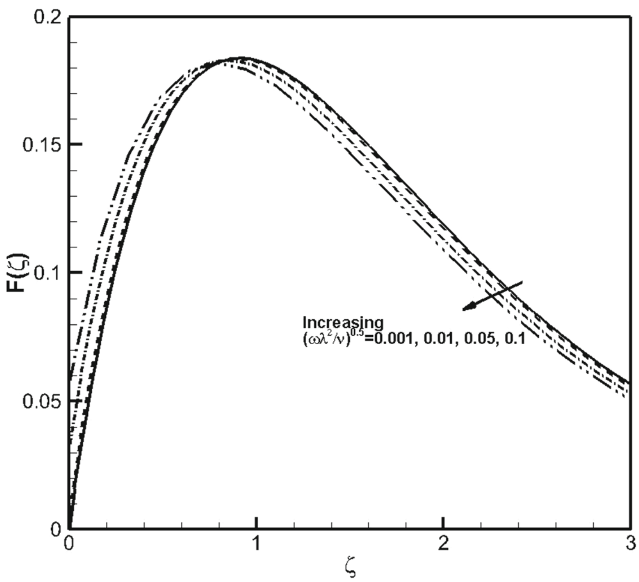

Fig. 6 Radial velocity profiles with various slip B.C.s

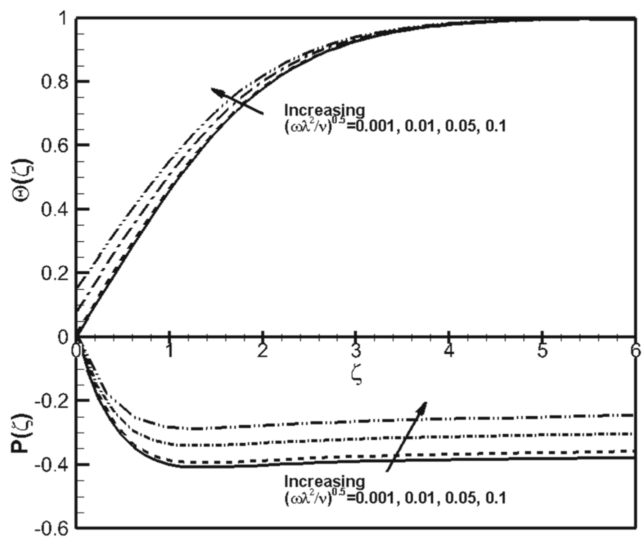

Fig. 8 Pressure and temperature effects on velocity components

Figure 8 shows the changes of the temperature and pressure with different degree of rarefaction. While previous studies [29] relied on the change of the Kn number, this work displays the changes in the temperature-jump with different $\sqrt{\omega\lambda^2/\nu}$. At the disk surface, the gas temperature approaches to the free stream value with reduced heat flux. The temperature profiles display an asymptote of unity, whether the B.C.s are slip/jump or not. The pressure profiles in Fig. 8 are affected by the velocity-slip B.C.s. The asymptotes for each of the cases decrease in a considerable higher proportion compared with those for the velocities. The proposed solutions reflect that the influence of the disk movement is dwarfed under velocity-slip B.C.s. Consequently, the pressure of the flow upstream decreases as the effects of the velocity-slip become more significant. Far from the rotating disk with negligible viscous effect, and for an incompressible flow, along a single streamline, the total pressure shall remain constant, following the Bernoulli equation:

$$p + \frac{1}{2}\rho V^2 = Constant, \tag{22}$$

then, the pressure is restricted to the changes in velocity components. An overall increment in the angular velocity creates an increment in both p and V. However, as stated

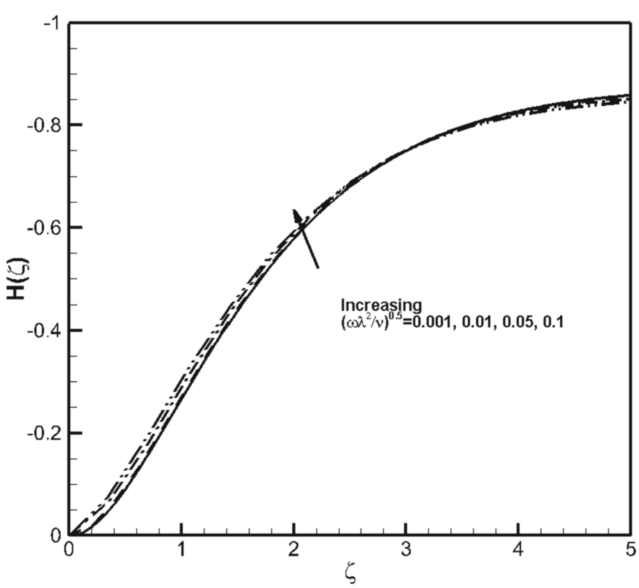

Fig. 7 Axial velocity profiles with various slip B.C.s

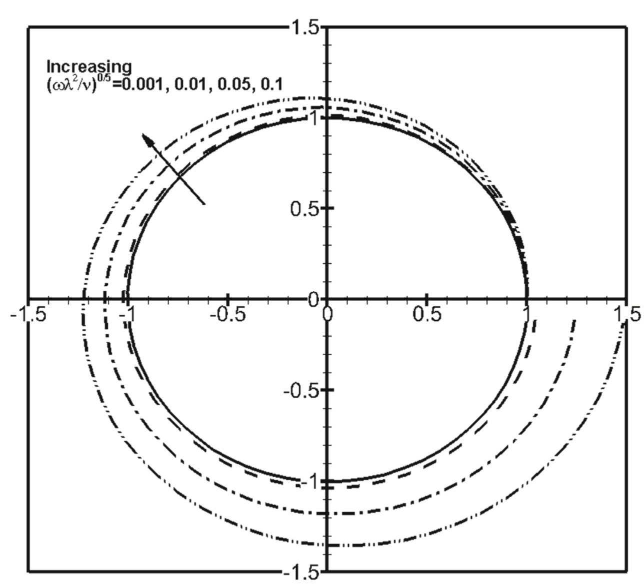

Fig. 9 Streamlines for particles at the disk surface

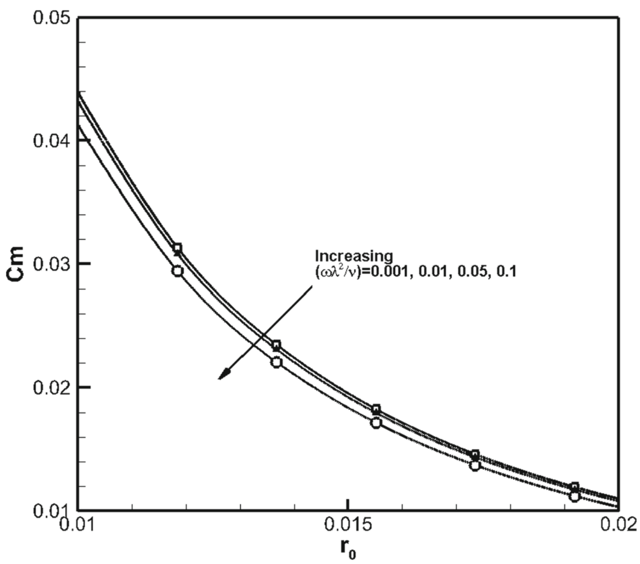

Fig. 10 Torque coefficients with different velocity slip B.C.s

in (6), the terms for $P(\zeta)$ and $G(\zeta)$ shall decrease in order to maintain the behavior of the previous equations. These effects are reflected in Figs. 5 and 8.

The stream function, introduced in (19), is solved with different degrees of rarefaction. Figure 9 presents the solutions for the stream lines at the disk surface. The curves are from (19), where $k_1 = 1$ for a particle movement starting at $r(\theta = 0) = 1$. The stream functions vary with different slip conditions. The curves tend to open their trajectories into a spiral form. Different from the circular trajectories expected in the nonslip flow, these effects of (14) are more noticeable at higher values of $\sqrt{\omega\lambda^2/\nu}$.

Finally, Fig. 10 presents the solution to (21). The torque coefficient and viscous drag decrease as rarefaction increases [19]. In consequence, the transmission of movement to the flow is less effective.

4 Summary

In this paper, an analysis of rarefied flows over a rotating disk is presented. The velocity, temperature, and pressure profiles are computed with several ODEs and velocity-slip and temperature-jump B.C.s with the shooting method, not some finite difference methods in the literature. Compared with non-slip viscous flows, velocities at the disk surface increase and the peak values in the radial velocity profile shift towards the disk. As a consequence, many velocity profile cross-overs happen. Due to the temperature jump at the disk surface, the gas temperature approaches to the free stream value with a reduced heat flux. Streamlines at the disk surface are shown, and they present the effects of the velocity-slip at the disk surface. Rarefaction effects are proven to be a factor in the decrement of the influence of the disk.

The results can find many applications where near continuum flows exist.

References

1. M. Matthews, Y.M. Stokes, Lubrication analysis and numerical simulation of the viscous Micropump with slip. Int. J. Heat Fluid Flow **33**(1), 22–34 (2012)
2. T. Zhang, P. Zhang, C.K. Law, Q. Fei, Chem. Vap. Depos. (2009)
3. N.T. Nguyen, X.Y. Huang, T.K. Chuan, MEMS-micropumps: a review. J. Fluids Eng. **124**, 384 (2002)
4. I.V. Shvchuk, *Convective heat and mass transfer in rotating disk systems*, 1st edn. (Springer, Berlin, 2009)
5. P. Ligrani, D. Blanchard, B. Gale, Slip due to surface roughness for a newtonian liquid in a viscous microscale disk pump. Phys. Fluids **22**, 5 (2010). doi:10.1063/1.3419081
6. W. Vincenti, C. Kruger, *An introduction to physical gasdynamics*, 1st edn. (Wiley, 1965)
7. N. Bachok, A. Ishak, I. Pop, Phys. B. (2011)
8. U.A. Paulus, T.J. Schmidt, H.A. Gasteiger, R.J. Behm, J. Electroanal. Chem. **2**, 495 (2001)
9. H. Schlichting, K. Gersten, *Boundary Layer Theory*, 6th edn. (McGraw-Hill, 1992)
10. F.M. White, *Viscous fluid flow*, 3rd ed (McGraw-Hill, 2006)
11. D.M. Hannah, *Forced flow against a rotating disk*, 1st edn. (H.M. Stationery Office, 1952)
12. B. Shaoo, S. Abbasbandy, S. Poncet, A brief note on the computation of the bodewadt flow with navier slip boundary conditions. Comput. Fluids **90**, 133–137 (2014)
13. K. Methta, K.N. Rao, Boundary layer flow over a rotating permeable plane. J. Phys. Soc. Jpn. **63**(6), 2149–2156 (1994)
14. P.J. Zanbergen, D. Dijkstta, Von Karman swirling flows. Annu. Rev. Fluid Mech. **19**, 465–491 (1987)
15. W.G. Cochran, The flow due to a rotating disk. Proc. Cambridge Philos. Soc. **30**, 365–375 (1934)
16. E.R. Benton, On the flow due to a rotating disc. J. Fluid Mech. **24**, 781–800 (1966)
17. K. Millsaps, K. Polhhausen, Heat transfer by laminar from a rotating plate. J. Aeronaut. Sci. **19**, 120–126 (1952)
18. E.M. Sparrow, J.L. Gregg, Heat transfer from a rotating disk to fluids of any Prandtl number. ASME J. Heat Transf. **81**, 249–251 (1959)
19. M. Miklavcic, C.Y. Wang, The flow due to a rough rotating disk. Zeitschrift Fur Angewandte Mathmatik Und Physik **55**(2), 235–246 (2004)
20. A. Arikoglu, I. Ozkol, Analysis for slip flow over a single free disk with heat transfer. J. Fluids Eng. **127**(3), 624–627 (2005)
21. A. Pantokratoras, A common error made in investigation of boundary layer flows. Appl. Math. Model. **33**(1), 413–422 (2009)
22. J.K. Zhou, *Differential transformation and its application for electrical circuits* (Huazhong Univ. Press, Wuhan, 1986)
23. E. Osalusi, J. Side, R. Harris, The effects of ohmic heating and viscous dissipation on unsteady MHD and slip flow over a porous rotating disk with variable properties in the presence of hall and ion-slip current. Int. Commun. Heat Mass Transf. **34**, 1017–1029 (2007)
24. E.H. Kennard, *Kinetic Theory of Gases* (McGraw-Hill, 1939)
25. M.N. Kogan, *Rarefied gas dynamics* (Plenum Press, 1969), pp. 386–400

26. M.V. Smoluchowski, Stzber, Akad, Wiss Wien (Ab, 2a), 107 (1898) pp.304 (1898); 108, pp. 5 (1899)
27. A.A. Kendoush, J Heat Transf. **2**, 135 (2013)
28. D. Blanchard, P. Ligrani, Slip and accommodation coefficients from rarefication and roughness in rotating microscale disk flows. Phys. Fluids **19**, 063602 (2007)
29. A. Arikoglu, G. Komurgoz, A. Gunes, Effect of second-order velocity slip and temperature jump conditions on rotating disk flow in the case of blowing and suction with entropy generations. Heat Trans. Res. **45**(2), 171–198 (2004)
30. A. Arikoglu, G. Komurgoz, I. Ozkol, Effect of slip on the entropy generation from a single rotating disk. J. Fluids Eng. **130**, 10 (2008). Article Number: 101202
31. J.D. Sherwood, Resistance coefficients for stokes flow around a disk with a navier slip condition. Phys. Fluids **9**, 24 (2012)
32. S. Rao, *Applied numerical methods for engineers and scientists*, 1st edn. (Prentice Hall, 2002)
33. D.G. Barbee, P.H. Newell, T. Shih, J. Aircr. **8**, 8 (1971)
34. R. Holsapple, R. Venkataraman, D. Doman, A modified simple shooting method for solving two-point boundary-value problems. (No. AFRL-VA-WP-TP-2002-327). Air Force Research Lab Wright-Patterson AFB OH Air Vehicles Directorate (2002)
35. I. Faragó, *Numerical Methods for ordinary differential equations*, 1st edn. (Tankönyvtár, 2014)
36. A. Kaw, *Shooting Method* (University of South Florida, 2009)